J Antimicrob Chemother 2022; **77**: 1710–1719
https://doi.org/10.1093/jac/dkac103 Advance Access publication 25 April 2022

Journal of Antimicrobial Chemotherapy

Drug concentration at the site of disease in children with pulmonary tuberculosis

Elisa Lopez-Varela [1,2]*†, Ahmed A. Abulfathi [3,4,5]†, Natasha Strydom[6]†, Pierre Goussard[7], Abraham C. van Wyk[8], Anne Marie Demers[1,9], Anneen Van Deventer[1], Anthony J. Garcia-Prats [1,10], Johannes van der Merwe[3], Matthew Zimmerman[11], Claire L. Carter[11,12], Jacques Janson[13], Julie Morrison[7], Helmuth Reuter[3], Eric H. Decloedt [3], James A. Seddon[1,14], Elin M. Svensson[15,16], Rob Warren[17], Radojka M. Savic[6], Véronique Dartois[11]‡ and Anneke C. Hesseling[1]‡

[1]Desmond Tutu TB Centre, Department of Paediatrics and Child Health, Faculty of Medicine and Health Sciences, Stellenbosch University, Cape Town, South Africa; [2]ISGlobal, Barcelona Centre for International Health Research (CRESIB), Hospital Clínic - Universidad de Barcelona, Barcelona, Spain; [3]Division of Clinical Pharmacology, Department of Medicine, Faculty of Medicine and Health Sciences, Stellenbosch University, Cape Town, South Africa; [4]Department of Clinical Pharmacology and Therapeutics, Faculty of Basic Clinical Sciences, College of Medical Sciences, University of Maiduguri, Maiduguri, Nigeria; [5]Center for Pharmacometrics & Systems Pharmacology, Department of Pharmaceutics, College of Pharmacy, University of Florida, Orlando, USA; [6]Department of Bioengineering and Therapeutic Sciences, University of California San Francisco, San Francisco, California, 94158, USA; [7]Department of Paediatrics and Child Health, Faculty of Medicine and Health Sciences, Stellenbosch University, Cape Town, South Africa; [8]Division of Anatomical Pathology, Tygerberg Hospital, National Health Laboratory Service, Faculty of Medicine and Health Sciences, Stellenbosch University, Cape Town, South Africa; [9]Service de microbiologie, Département clinique de médecine de laboratoire, Centre Hospitalier Universitaire Sainte-Justine, Montreal, Canada; [10]Department of Pediatrics, University of Wisconsin School of Medicine and Public Health, Madison, WI, USA; [11]Center for Discovery and Innovation, Hackensack Meridian Health, New Jersey, USA, and Department of Medical Sciences, Hackensack School of Medicine, Nutley, New Jersey, USA; [12]Department of Pathology, Hackensack School of Medicine, Nutley, New Jersey 07110, USA; [13]Division of Cardiothoracic Surgery, Department of Surgery, Faculty of Medicine and Health Sciences, Stellenbosch University, Cape Town, South Africa; [14]Department of Infectious Diseases, Imperial College London, London, UK; [15]Department of Pharmacy, Uppsala University, Uppsala, Sweden; [16]Department of Pharmacy, Radboud Institute for Health Sciences, Radboud University Medical Center, Nijmegen, The Netherlands; [17]DST/NRF Centre of Excellence for Biomedical Tuberculosis Research/South African Medical Research Council Centre for Tuberculosis Research, Division of Molecular Biology and Human Genetics, Faculty of Medicine and Health Sciences, Stellenbosch University, Cape Town, South Africa

*Corresponding author: E-mail: elisa.lopez@isglobal.org
†These authors made an equal contribution.
‡These authors made an equal contribution.

Received 28 November 2021; accepted 7 March 2022

Background: Current TB treatment for children is not optimized to provide adequate drug levels in TB lesions. Dose optimization of first-line antituberculosis drugs to increase exposure at the site of disease could facilitate more optimal treatment and future treatment-shortening strategies across the disease spectrum in children with pulmonary TB.

Objectives: To determine the concentrations of first-line antituberculosis drugs at the site of disease in children with intrathoracic TB.

Methods: We quantified drug concentrations in tissue samples from 13 children, median age 8.6 months, with complicated forms of pulmonary TB requiring bronchoscopy or transthoracic surgical lymph node decompression in a tertiary hospital in Cape Town, South Africa. Pharmacokinetic models were used to describe drug penetration characteristics and to simulate concentration profiles for bronchoalveolar lavage, homogenized lymph nodes, and cellular and necrotic lymph node lesions.

Results: Isoniazid, rifampicin and pyrazinamide showed lower penetration in most lymph node areas compared with plasma, while ethambutol accumulated in tissue. None of the drugs studied was able to reach target concentration in necrotic lesions.

Conclusions: Despite similar penetration characteristics compared with adults, low plasma exposures in children led to low site of disease exposures for all drugs except for isoniazid.

Introduction

Adequate exposure of antituberculosis drugs at the site of disease is required for sterilization of tuberculous lesions. Only half of the one million children estimated to have TB are treated each year.[1] Those who do receive treatment are often underdosed using current weight-based treatment guidelines.[2] Children typically have lower plasma concentrations for the same milligrams per kilogram dose compared with adults for most first-line antituberculosis drugs, particularly for rifampicin, an important sterilizing drug.[3] Additionally, young children, those with the highest risk of TB, are also at risk of developing more severe forms of TB, with increased mortality.

The treatment of paediatric intrathoracic TB (the most common form of TB in children, occurring in >75% of cases), including drug regimens, dosing and treatment duration, has historically been extrapolated from efficacy trials in adults, with limited consideration of differences in the clinical spectrum of disease or the pharmacokinetic (PK) variability observed in children. While many children with TB have paucibacillary disease limited to the mediastinal lymph nodes (LN), many (up to 40%) have more extensive forms of disease, including miliary TB, parenchymal pathology or complicated LN involvement with breakthrough to endobronchial disease.[4] Although a shorter treatment of 4 months at standard doses was recently shown to be non-inferior to the currently recommended first-line 6 months treatment in children with non-severe intrathoracic and extrathoracic LN disease in the SHINE trial,[5] children with TB currently still receive the same regimen, regardless of disease spectrum, severity and bacillary burden.

Antituberculosis drug dosing is based on target drug concentrations measured in plasma, despite evidence showing a low correlation between drug concentration measured in plasma versus at sites of disease, where penetration may be both lesion- and drug-specific.[6,7] To date, few studies in humans have evaluated the penetration of drugs into intrathoracic TB lesions. The limited studies to date have been in adults and have focused on lung tissue,[6,8–10] despite the fact that TB can be thought of as a lymphatic disease.[11]

Understanding drug exposure at the site of disease could facilitate the design of more-effective and potentially shorter regimens in children across the disease spectrum, and may have broader therapeutic implications, including for adults. We aimed to characterize the concentrations of first-line antituberculosis drugs at the site of disease in children with complicated intrathoracic TB requiring bronchoscopy or surgical LN decompression (SD), and to compare drug exposures in children with adult levels in plasma and lesions, against current targets correlated with efficacy.[6,7,12–20]

Patients and methods

Study design and setting

From November 2018 through March 2019, we prospectively enrolled children with complicated intrathoracic TB routinely referred to Tygerberg Hospital, Cape Town, South Africa. Children underwent bronchoscopy or transthoracic surgical LN decompression (SD) for diagnosis or to establish airway patency. Children were eligible if they were on a rifampicin-containing regimen for at least 10 days.

Ethics statement

The Health Research Ethics Committee at Stellenbosch University (N18/05/059) approved this study. Written informed consent was obtained from parents/legal guardians.

Clinical procedures

On the day of the procedure, antituberculosis treatment was administered by the study team after an overnight fast. The study was designed to ensure that different participants contributed samples at different timepoints, from peak plasma to the end of the distribution phase, to reconstruct the PK profile at the site of disease, with dosing times planned at 2 h before SD, or randomized to 2, 4 or 6 h prior to bronchoscopy. Randomization in the SD group was not feasible owing to the complexity and duration of the procedure. Treatment consisted of weight-banded once-daily oral doses of isoniazid (10–15 mg/kg), rifampicin (10–20 mg/kg) and pyrazinamide (30–40 mg/kg) using fixed-dose dispersible paediatric combinations (Table S1, available as Supplementary data at *JAC* Online). Ethambutol (15–25 mg/kg) was added in children who were HIV-coinfected and at clinical discretion.[21,22] Children with significant airway obstruction received oral prednisone (2 mg/kg daily).

Plasma and tissue sampling

Venous or arterial blood samples were collected pre-dose, and at approximately 2, 4 and 6 h post-dose. Blood sampling was targeted to be coupled to the site of disease sample and was recorded in relation to the time of bronchoscopy/SD. Bronchoalveolar lavage (BAL) samples were taken from children undergoing bronchoscopy and, when available, endobronchial LN biopsy specimens were collected for PK analysis and microbiological investigation. Lymph node tissue samples were collected during SD for PK, histology and microbiology. Depending on the size and consistency of lymph node fragments, samples were collected in either homogenizing tubes or in Cryomold for PK analysis. Further details are described in the Supplementary data.

Analytical methods

Assays to quantify rifampicin, isoniazid, pyrazinamide and ethambutol concentrations in plasma, BAL and LN tissue used validated methods.[6] Plasma and BAL samples were analysed using a validated high-performance liquid chromatography-tandem mass spectrometry (LC-MS/MS) assay.[6,8] LN material obtained through endobronchial biopsy

and liquefied LNs from SD were analysed using previously described validated LC-MS/MS methods.[6,8] Solid SD specimens larger than 5 mm were further classified by histology on frozen section into cellular, necrotic, and mixed lesions (cellular with necrosis in the background). For these specimens, drug concentrations were measured from pathologically distinct regions using laser capture microdissection (LCM) combined with LC-MS/MS as previously described.[8]

PK modelling and simulations

Published rifampicin, isoniazid and pyrazinamide population PK models in children, and an adult ethambutol model, were optimized, and the final models were fit to the new data.[23,12] All drug PK models included weight-based allometric scaling on clearance and volume, and for rifampicin and isoniazid, included postmenstrual age as a covariate on clearance.[23] To model ethambutol in children, South African adult PK parameters from Jönsson *et al*.[12] were scaled allometrically to the children's weights. The parameters from these models were fixed and the model fit evaluated and subsequently re-estimated where necessary.

Using an established method,[7] site of disease PK was described by equation 1 where each lesion compartment was linked to the plasma PK model (see Figure S1).

$$\frac{dC_{SOD}}{dt} = k_{pl-SOD} \times \left(R_{SOD-pl} \times \frac{A_{plasma}}{V_{plasma}} - C_{SOD} \right) \quad (1)$$

C_{SOD} represents the drug concentration in LNs or BAL, k_{pl-SOD} are intercompartment rate constants for the transfer of drug from the plasma to the site of disease, R_{SOD-pl} are the penetration coefficients between site of disease and plasma, and A_{plasma}/V_{plasma} is the drug concentration in plasma at time t.

Concentration–time profiles and derived area under the concentration–time curve from 0 to 24 h (AUC_{0-24}) at steady-state were simulated for the median age and weight of children in the cohort (8.6 months, 8.2 kg) using our cohort plasma and tissue estimates. To compare these outputs with adult exposure from the same population, we used published population PK models from South African adults for rifampicin, isoniazid, pyrazinamide and ethambutol.[12–15] Concentration profiles for the four drugs in the different compartments were compared with appropriate inhibitory and bactericidal target concentrations. We used published distributions of wild-type MIC for plasma, BAL, homogenized LN and mixed tissue, intracellular macrophage IC_{50} for cellular lesions, and caseum MBC for necrotic tissue or caseum (Table S2). Further details are described in the Supplementary data.

Data sharing

Data underlying these findings may be requested from the corresponding author.

Results

Participant characteristics

We enrolled 13 children who collectively underwent 15 procedures including eight bronchoscopies and seven SDs to resolve severe airway obstruction due to complicated TB. Baseline clinical and radiological characteristics are shown in Table 1, and individual participant characteristics in Table S3. All children had evidence of severe extensive intrathoracic disease on chest imaging (Figure S2). All were bacteriologically confirmed; one child had isoniazid monoresistant TB and a second had multidrug-resistant TB which was only diagnosed following the procedure.

Table 1. Patient characteristics at the time of procedure by study group in children with complicated pulmonary tuberculosis

Characteristic	Bronchoscopy ($N=8$)	Surgical decompression ($N=7$)
Male sex, *n* (%)	3 (37.5)	4 (57.1)
Median age, months (IQR)	17.6 (6.3–41.0)	6.9 (3.4–17.2)
Median weight, kg (IQR)	9.9 (8.2–12.4)	7.1 (4.1–8.3)
Median weight-for-age Z-score[a] (IQR)	0.1 (−1.3 to 0.8)	−1.0 (−4.2 to −0.1)
HIV-positive[b], *n* (%)	1 (12.5)	0 (0.0)
Child has current TB source case, *n* (%)	5 (62.5)	5 (71.4)
TB disease type, *n* (%)		
PTB only	6 (75.0)	6 (85.7)
PTB and EPTB[c]	2 (25.0)	1 (14.3)
Previous TB episode, *n* (%)	1 (12.5)	0 (0.0)
Median days on treatment (IQR)	64 (60–73)	34 (28–74)
Regimen, *n* (%)		
HR[d]	2 (25.0)	0 (0.0)
HRZ[e]	2 (25.0)	1 (14.3)
HRZE	3 (37.5)	5 (71.4)
RZEL[f]	1 (12.5)	1 (14.3)
Median dose, mg/kg (IQR)		
Rifampicin	12.8 (12.1–16.0)	12.3 (11.1–15.0)
Isoniazid	12.8 (11.4–14.8)	12.2 (11.1–12.7)
Pyrazinamide	28.5 (23.8–30.9)	30.5 (25.3–34.2)
Ethambutol	20.2 (18.6–22.8)	20.8 (20.2–24.1)
Receiving oral steroids, *n* (%)	6 (75.0)	7 (100.0)
Chest X-ray characteristics, *n* (%)		
Consolidation	7 (87.5)	4 (57.1)
Collapse	3 (37.5)	1 (14.3)
Cavity	1 (12.5)	0 (0.0)
Paratracheal nodes	3 (37.5)	4 (57.1)
Hilar nodes	6 (75.0)	5 (71.4)
Airway compression	6 (75.0)	6 (85.7)
Pleural effusion	1 (12.5)	0

Abbreviations: EPTB, extrapulmonary TB; PTB, pulmonary TB; H, isoniazid; R, rifampicin; Z, pyrazinamide; E, ethambutol; L, levofloxacin.
[a]Anthropometric Z scores were calculated based on WHO growth standards.
[b]HIV-infected child on abacavir, lamivudine and Lopinavir/ritonavir.
[c]EPTB included: group 1– disseminated ($N=1$) and miliary ($N=1$); group 2– abdominal ($N=1$).
[d]One case without prior bacteriological confirmation was diagnosed with multidrug-resistant TB detected on the day of the procedure.
[e]One child received HRZ plus ethionamide for disseminated disease.
[f]One case of isoniazid mono-resistance diagnosed at the time of TB treatment initiation.

Plasma and tissue samples

LN samples were obtained in 4/8 (50%) of the bronchoscopy cases through endobronchial biopsy, and in all seven (100%) SD cases (Table S3). Histological examination of all SD tissue

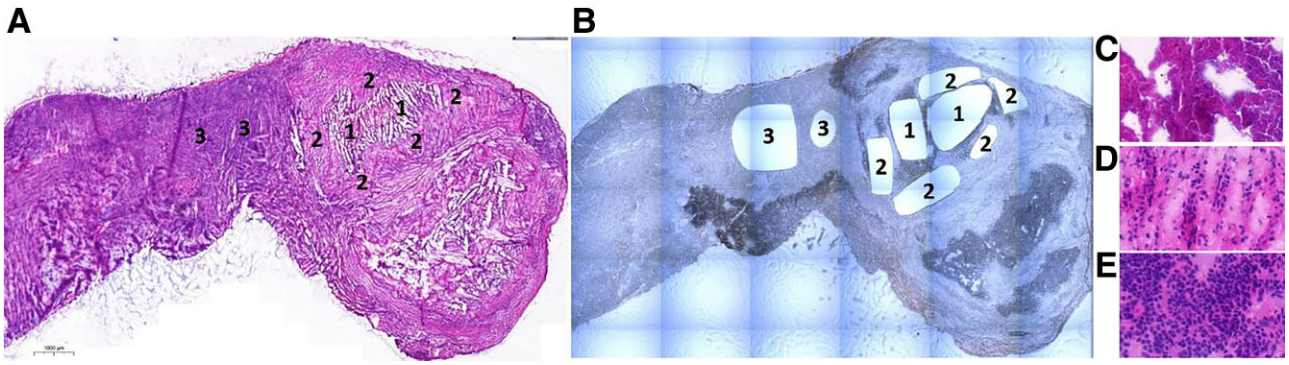

Figure 1. Laser capture microdissection in a representative lymph node specimen. Haematoxylin and eosin-stained lymph node (frozen section) containing two lesions (A) and its corresponding serial section taken for laser capture microdissection (B). Regions 1–3 represent the areas dissected for drug quantification by LC-MS/MS. Example histology of the different areas dissected are shown and correspond to necrotic areas of the lesion (A, B1 and C), the cellular layer of the lesion (A, B2 and D), and a lymphocyte rich region (A, B3 and E). This figure appears in colour in the online version of *JAC* and in black and white in the print version of *JAC*.

fragments showed that most specimens were characterized by necrotizing granulomatous inflammation. None to minor residual normal tissue was identified in LNs, and only one had preserved architecture displaying reactive follicular hyperplasia. Ziehl-Neelsen staining revealed acid-fast bacilli in four of the seven samples, of which two had numerous bacilli, which were more abundant in necrotic foci. While none of the BAL samples was culture-positive, 4/7 SD cases were culture-positive. MICs were obtained for two of the Mtb isolates and values were within normal MIC range (Table S3).

The concentrations of rifampicin, isoniazid, pyrazinamide and ethambutol were measured in 44 plasma, and in 65 BAL and LN samples collected at 2 to 8 h post-dose. Drug concentrations in BAL could only be determined in 4/8 (50%) children due to urea concentrations below the limit of quantification in BAL, a requirement for dilution factor calculation. LCM was performed in nine frozen LN specimens from four participants, allowing for the spatial quantification of drugs within the spectrum of different tissue compartments identified (necrotic, cellular, or mixed lymphoid) (Figure 1). The longitudinal PK profiles showed that there was large variability in the concentrations of all drugs amongst tissue compartments, between participants, and within similar lesions in the same participant (Figure 2).

Modelling of plasma PK and tissue distribution

Model building used prior published paediatric population PK models and estimates for the plasma PK model were similar to published parameters (Table S4). The final PK estimates are shown in Table 2. The rate and penetration coefficient estimates for each drug are shown in Table 3. Simulated PK profiles with their relevant concentration targets and AUC_{0-24} values for tissue compartments are shown in Figure S3 and Table S5, respectively.

Rifampicin

Rifampicin had high exposure in cellular tissue with higher concentration and AUC_{0-24} levels compared with plasma. Modelling results showed a penetration coefficient of 1.37 (95% CI: 0.87–1.87) for cellular tissue. Necrotic regions had the lowest rifampicin concentrations and the lowest penetration coefficient (0.55, 95% CI: 0.477–0.641). Rifampicin concentrations were below the upper end of the MIC range for >50% of the dosing interval in all tissue compartments except necrotic regions (Figure S3).

Isoniazid

Isoniazid had good penetration into necrotic tissue with an estimated penetration coefficient of 0.84 (95% CI: 0.80–0.88), but did not reach the high caseum MBC (casMBC) target of 128 mg/kg. The penetration coefficient was lower in the cellular region of granulomas (0.56, 95% CI: 0.32–0.79), but concentration levels were above the MIC for 75% of the 24 h dosing profile. Overall, isoniazid exposure was above the MIC for approximately 50% of the dosing interval for all tissue compartments except necrotic lesions.

Pyrazinamide

Drug penetration coefficient estimates were relatively low and similar for cellular (0.42, 95% CI: 0.36–0.48) and necrotic lesions (0.40, 95% CI: 0.30–0.50). Despite low plasma pyrazinamide concentrations, our simulations showed pyrazinamide exposure was above the 'acidic' macrophage MIC for approximately 54% of the dosing interval in cellular compartments and below target casMBC for necrotic lesions.

Ethambutol

High penetration into all compartments was observed for ethambutol, and penetration coefficients ranged from 1.11 (95% CI: 0.43–1.95) in necrotic lesions, to 6.17 (95% CI: 0.91–14.4) in cellular tissue. In all compartments except for necrotic lesions, ethambutol appeared to accumulate in tissue. However, similar to other first-line drugs, ethambutol concentrations were never higher than its casMBC target and in other tissue types were above the lower range of their respective targets for only 29%–50% of the dosing interval.

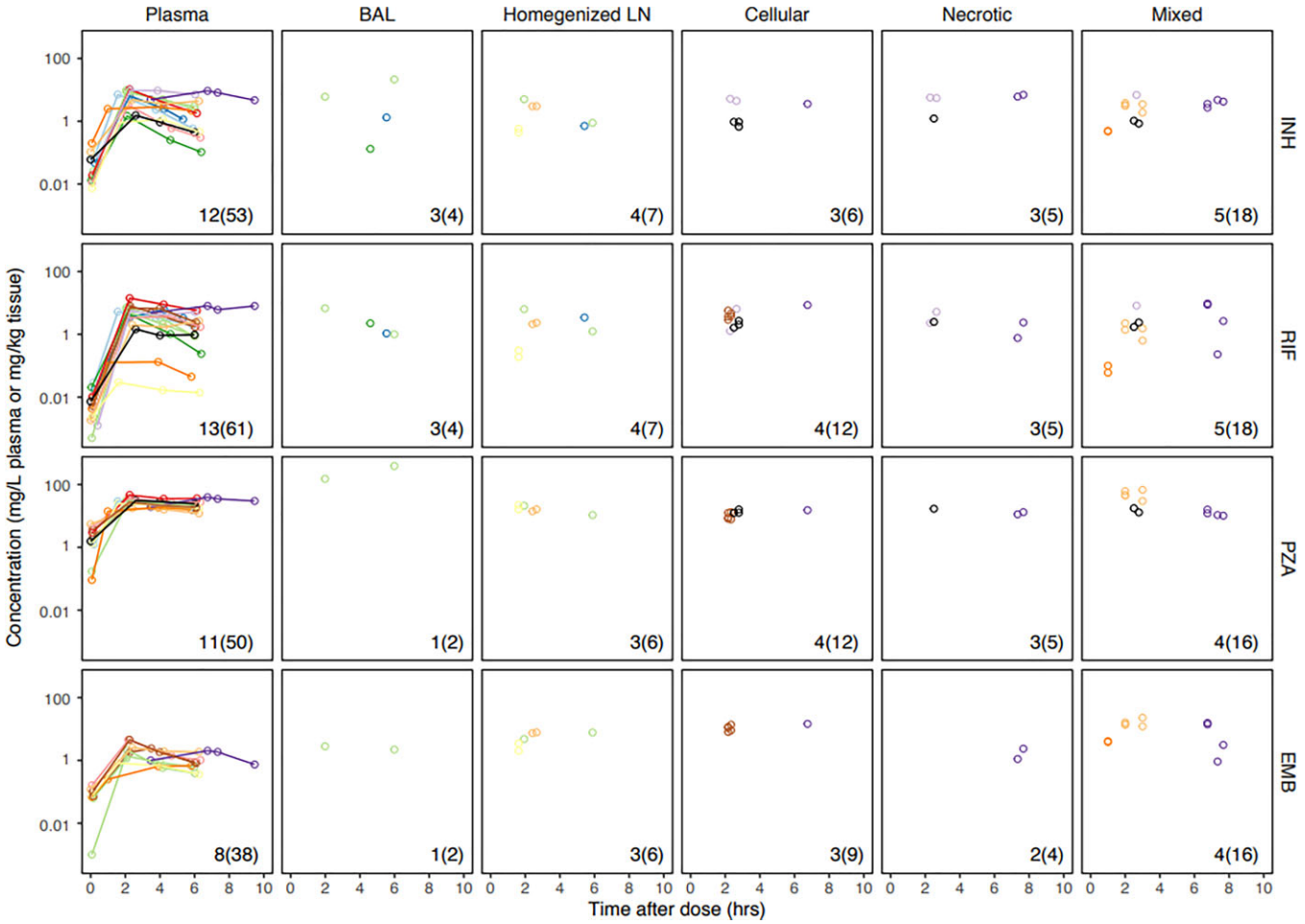

Figure 2. Raw PK data for each drug in each lesion type. Log-scale concentration–time profiles are shown for five lesion types and four drugs by respective panel. Plasma concentrations over time for each individual were measured at multiple timepoints after the time of drug administration and before bronchoscopy or surgical decompression and are shown as individual lines of different colours. Lesion concentrations were measured at a single timepoint (time of resection) per subject and are represented by circles of different colours that correspond to their individual subject plasma line. The number of patients (and observations) for each lesion and drug are shown in the bottom, right corner of each image. Abbreviations: BAL, bronchoalveolar lavage; LN, lymph node; INH, isoniazid; RIF, rifampicin; PZA, pyrazinamide; EMB, ethambutol. This figure appears in colour in the online version of *JAC* and in black and white in the print version of *JAC*.

Paediatric exposures compared with adult predictions

Penetration coefficient values for necrotic lesions were similar between children and adults (Table 3). Additional simulations to compare first-line drug concentration–time profiles of lesions in adults and children are shown in Figure 3. Mean values of the simulated steady-state AUC_{0-24} in children compared with adults for plasma, cellular and necrotic lesions are shown in Table 4.

Plasma rifampicin exposures were similar to adult reference values (AUC_{0-24} of 41.7 versus 38.3 mg·h/L).[15] However, only 15% of the 1000 simulated rifampicin AUC_{0-24} in plasma were above the proposed adults target of approximately 42 mg·h/L.[24–26] Children did appear to have more favourable drug penetration in LNs compared with penetration into lung lesions observed in adults, particularly in cellular regions, where the penetration coefficient was 1.37 (95% CI: 0.874–1.87) resulting in an AUC_{0-24} of 55.2 mg·h/L.

Isoniazid plasma concentrations were similar in children compared with the simulated adult values (AUC_{0-24} of 25.3 versus 27.7 mg·h/L). Particularly low plasma pyrazinamide exposures were observed compared with adult data (AUC_{0-24} of 248 versus 466 mg·h/L) and resulted in children having approximately only half the exposure levels of adults in cellular and necrotic lesions. For ethambutol, the AUC_{0-24} in children was six-fold lower than the simulated adult value of 78.5 mg·h/L. There were no prior adult data on ethambutol concentrations at pulmonary site of disease to allow comparison with paediatric data.

Discussion

We report for the first time, data on drug concentrations and exposure into intrathoracic LNs and BAL in children with severe intrathoracic TB. Penetration into the site of disease was similar in children compared with adults. However, the standard

Table 2. Final plasma pharmacokinetic parameters of first-line antituberculosis drugs in children with complicated pulmonary tuberculosis

Parameter	Isoniazid	Rifampicin	Pyrazinamide	Ethambutol
Tlag (h)	0.4 (1.00)	0.961 (14.3)	NA	0.493 (13.8)
k_a (h^{-1})	0.654 (15.1)	0.592 (13.3)	0.586 (14.9)	0.324 (7.00)
CL/F (L/h)	7.36 (29.8)	4.64 (8.90)	0.977 (9.90)	15.8 (18.0)
Vc/F (L)	8.72 (36.8)	8.27 (11.2)	5.23 (13.3)	8.59 (5.60)
Q (L/h)	0.0751 (76.2)	NA	NA	7.65 (2.30)
Vp/F (L)	12.1 (59.5)	NA	NA	87.2 (2.30)
TM50 (weeks)	49.0 (FIXED)	58.2 (FIXED)	NA	NA
Hill	2.19 (FIXED)	2.21 (FIXED)	NA	NA
IIV CL/F	0.817 (41.5)	0.187 (47.9)	0.0538 (59.7)	0.24 (36.8)
IIV Vc/F	NA	0.48 (48.3)	0.0629 (68.2)	NA

Abbreviations: Tlag, lag in absorption time; NA, not applicable; k_a, rate of absorption; CL, clearance; Vc, central volume of distribution; Q, inter-compartmental clearance; Vp, peripheral volume of distribution; F, bioavailability; TM50, post-menstrual age at 50% of adult clearance; Hill, steepness of the maturation function; IIV, inter-individual variability. Parameters scaled to 8.6 month, 8.2 kg individual. Individual clearance and volume of distribution values were adjusted according to allometric scaling on weight, $CLi = CLstd \cdot (WT/8.2)^{0.75}$, $V1i = V1std \cdot (WT/8.2)^{1}$, $Qi = Qstd \cdot (WT/8.2)^{0.75}$, $V2i = V2std \cdot (WT/8.2)^{1}$.
Values in parentheses are the percentage relative standard error (RSE).

Table 3. Pharmacokinetic parameters of antituberculosis drugs according to the site of disease in children with pulmonary tuberculosis

		Ratio	
	Rate	Children estimate	Adult reference
Isoniazid			
BAL	20[a]	2.86 (1.53–2.91)	
Homogenized LN	20[a]	0.513 (0.28–0.75)	
Cellular	20[a]	0.556 (0.32–0.79)	[0.228] (0.223–0.233)
Necrotic	20[a]	0.843 (0.80–0.88)	[0.824] (0.776–1.01)
Mixed	2.58 (0.684–4.416)	0.486 (0.46–0.80)	
Rifampicin			
BAL	20[a]	1.13 (0.998–1.262)	
Homogenized LN	20[a]	1.17 (1.044–1.296)	
Cellular	0.639 (0.568–1.008)	1.37 (0.874–1.87)	[0.348] (0.122–0.574)
Necrotic	20[a]	0.552 (0.477–0.641)	[0.443] (0.251–0.635)
Mixed	20[a]	0.873 (0.725–1.07)	
Pyrazinamide			
BAL	0.218 (0.124–0.314)	20.4 (16–25)	
Homogenized LN	20[a]	0.753 (0.63–0.88)	
Cellular	20[a]	0.416 (0.36–0.48)	[0.698] (0.597–0.799)
Necrotic	20[a]	0.395 (0.30–0.50)	[0.394] (0.266–0.522)
Mixed	20[a]	1.4 (0.91–1.9)	
Ethambutol			
BAL	20[a]	1.34 (0.248–2.92)	
Homogenized LN	20[a]	3.16 (0.16–6.74)	
Cellular	0.574 (0.384–1.368)	6.17 (0.914–14.4)	
Necrotic	20[a]	1.11 (0.430–1.95)	
Mixed	20[a]	5.44 (2.15–10.5)	

Abbreviations: BAL, bronchoalveolar lavage; LN, lymph node; NA, not applicable.
The rate (kpl in h^{-1}, inter-compartmental rate constants for the transfer of drug from the plasma to the site of disease) and ratio (Rpl, the penetration coefficients (ratios) between site of disease and plasma) for each drug and site of disease are shown together with the adult ratio coefficient (Strydom *et al.*[7]) in parentheses, when available.
The following definitions were used for adult lesion: Cellular (defined as small cellular nodules); necrotic (caseum from closed nodule).
Values in parentheses are 95% CI. Values in square brackets are the adult reference.
[a]Values were fixed in model to assume an almost instantaneous penetration of the drug.

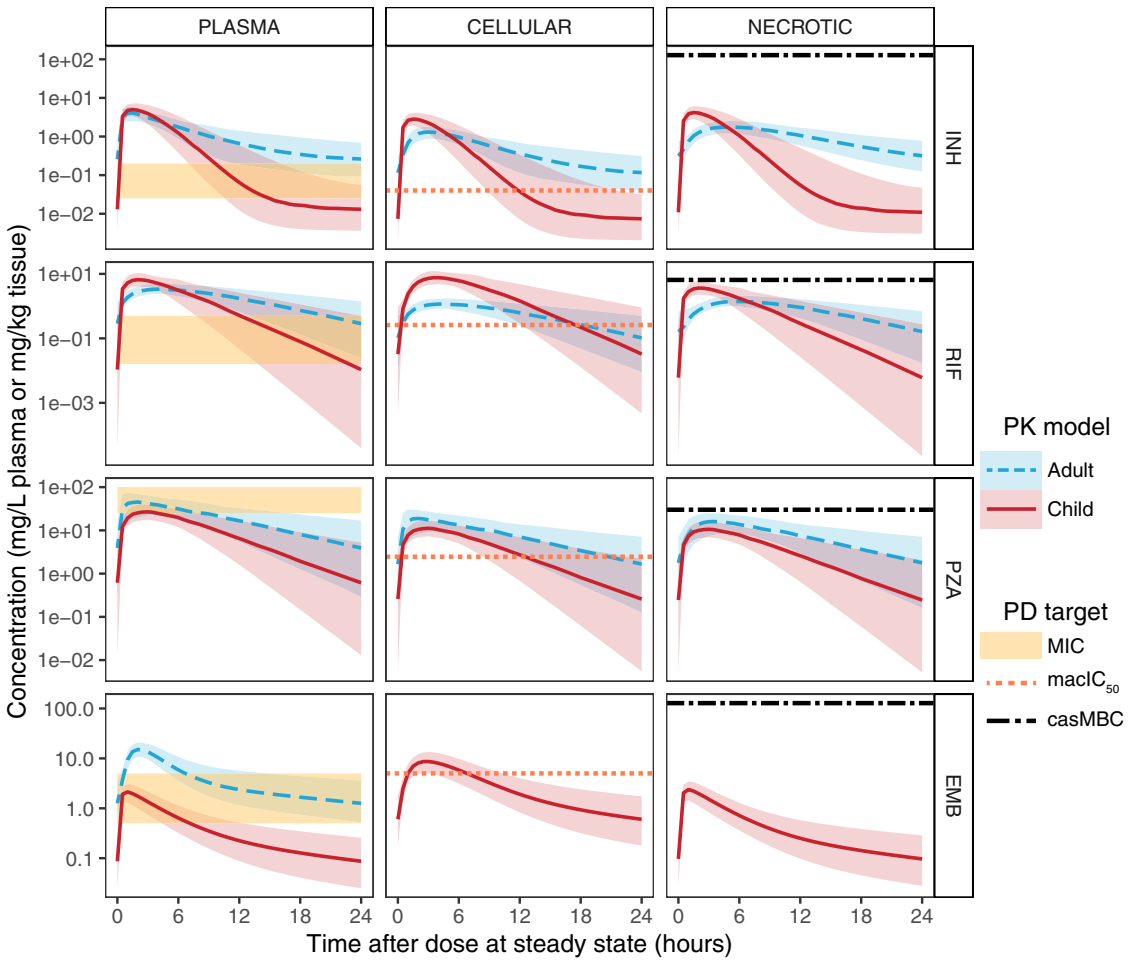

Figure 3. Simulated concentration–time profiles of children and adults relative to exposure target. Simulations for 1000 patients with the same representative characteristics were performed and their steady-state concentration–time profiles taken over 24 h. Red represents an 8.2 kg child aged 8.6 months with median and 95% CI. Blue represents simulated 60 kg adult profiles with available parameters from plasma [rifampicin (RIF; R), isoniazid (INH, H), pyrazinamide (PZA; Z) and ethambutol (EMB; E) from Smythe *et al*.,[15] Wilkins *et al*.[13,14] and Jönsson *et al*.,[12] respectively] and lesion parameters (from Strydom *et al*.[7]). Dosing for child was H = 120 mg, R = 120 mg, Z = 250 mg, E = 200 mg and for adult, H = 300 mg, R = 600 mg, Z = 1600 mg, E = 1100 mg. Yellow bands represent the distribution of PD exposure target selection: wild-type MIC for homogenized lymph node; intracellular macrophage IC_{50} for cellular lesions (orange dashed line) and caseum MBC for the necrotic tissue (black dashed line). Abbreviations: MBC, minimum bactericidal concentration. This figure appears in colour in the online version of *JAC* and in black and white in the print version of *JAC*.

WHO-recommended antituberculosis drug dosing resulted in low plasma and consequently, low site of disease exposures for all drugs except for isoniazid.

In our study, histopathological examination of SD tissue fragments showed predominantly necrotizing granulomatous inflammation, with little residual recognizable LN tissue. This was probably a reflection of the nature of the procedure (decompression rather than complete LN excision) and disease severity, as these LN were affected to the extent of causing airway compression. Acid-fast bacilli were seen on Ziehl-Neelsen staining in four of seven SD samples, including two that were acid-fast bacilli negative, after at least 4 weeks of TB therapy. Although Ziehl-Neelsen staining does not differentiate viable from non-viable organisms, it is possible that some viable organisms remained in LNs after more than a month of treatment. Bacilli were more numerous in necrotic foci. This is similar to data previously reported in animal models[27] and in human adults.[28]

The histological spectrum of the tissue samples between adults and children was similar, despite different excision locations. The penetration coefficients of necrotizing LNs in children were remarkably similar to those of adult lung granulomas, suggesting that penetration properties translate well between children and adults for these lesions. The penetration was highest for the two drugs with limited activity against quiescent mycobacteria: isoniazid and ethambutol. Conversely, the two drugs with sterilizing activity, rifampicin and pyrazinamide, had caseum exposures below their target concentrations (casMBC). A recent *ex vivo* model has shown that only rifampicin fully sterilizes bacilli in caseum,[29] with a casMBC of 6.5 mg/L. In the *in vivo* rabbit model of active TB, pyrazinamide was reported to exert bactericidal

Table 4. Area under the curve (0–24 h) values comparing exposure of first-line antituberculosis drugs in children compared with adults

		AUC_{0-24}, mg·h/L, median (95% CI)[a]		
Drug	Subject	Plasma	Cellular	Necrotic
Isoniazid	Adult[23]	27.7 (23.8–32)	11.8 (10.1–13.6)	23.3 (20–26.9)
	Child	25.3 (22.4–28.6)	10.8 (9.53–12.1)	21.6 (19.1–24.3)
Rifampicin	Adult[24]	41.7 (35.8–49.4)	14.5 (12.5–17.2)	18.5 (15.9–21.9)
	Child	38.3 (33.5–43.7)	55.2 (48.3–63)	21.2 (18.5–24.1)
Pyrazinamide	Adult[22]	466 (395–539)	194 (165–225)	184 (157–214)
	Child	248 (213–294)	103 (88.6–122)	97.9 (84.1–116)
Ethambutol	Adult[21]	105 (91.6–124)	NA	NA
	Child	12.3 (10.6–14.6)	76.8 (66.6–91.1)	13.7 (11.9–16.3)

Abbreviations: AUC_{0-24}, area under the curve from dosing time to 24 h after dose; NA, not applicable.
[a]Median of simulation of 1000 individuals with individual variability is shown with 95% CI. Adults received South Africa standard of care doses assuming 60 kg patient (doses were: rifampicin 600 mg; isoniazid 300 mg; pyrazinamide 1600 mg and ethambutol 1100 mg). Children were 8.2 kg and received: rifampicin 120 mg; isoniazid 120 mg; pyrazinamide 250 mg; ethambutol 200 mg.

activity on phenotypically drug-tolerant bacilli in hard-to-reach caseous lesions.[30]

We present, to our knowledge, the first human data on penetration of ethambutol into sites of disease compartments. Our results support the hypothesis that, despite its poor plasma-based PK/pharmacodynamic (PD) profile, the efficacy of ethambutol might be explained by the favourable penetration of this drug into TB lesions.[8] Despite being a polar drug,[31] ethambutol accumulated in all compartments relative to plasma and particularly in the cellular areas where ethambutol targets intracellular bacilli.[17] Overall, ethambutol exposures in different compartments were limited by the low plasma concentrations, which were significantly lower than in adults (C_{max} 2.3 versus 6.4 mg/L) and below the MIC target. This is consistent with previous paediatric studies, which showed erratic absorption and low concentrations of ethambutol in children dosed at 10–20 mg/kg per day.[32]

Given our results, antituberculosis treatment in children could benefit from higher ethambutol and rifampicin doses. The favourable penetration of ethambutol into LNs suggests that ethambutol should be dosed at 25 mg/kg (that is, at the higher end of the recommended 15–25 mg/kg) to achieve higher site of disease exposure. This dose is considered safe but doses beyond 25 mg/kg may be too high given ocular toxicity.[33] For rifampicin, only 15% of simulated plasma AUC_{0-24} in children reached the proposed adult target.[24–26] These data again emphasize the need for higher doses of rifampicin.[34] Low exposure to rifampicin is associated with worse treatment outcomes in children.[35–39] Several ongoing trials are evaluating higher doses of rifampicin of up to 50 mg/kg in adults, and short-term dosing of up to 70 mg/kg in children.[40] In accordance with the national guidelines at the time of the study, pyrazinamide was administered at 25 mg/kg rather than the current WHO recommended weight bands of 30–40 mg/kg. Higher dosing will likely improve time above the acidic MIC in cellular compartments but will still remain below the casMBC for necrotic lesions. We recommend that where possible pyrazinamide should be dosed at the higher end of its dosing range to maximize coverage in cellular lesions.

Future studies should include sample times that will better characterize the absorption phase of the drugs studied and later trough levels. For this initial study, the sample times were optimized around the planned medical procedure time and C_{max} to ensure measurable drug concentration. Peripheral volume and intercompartmental clearance estimates of isoniazid were not consistent with previously reported parameters. Data were collected only up to 6 h making this compartment difficult to parameterize. Therefore, isoniazid simulations used previously published PK parameters with lesion parameters from our model to ensure accurate prediction of terminal concentrations. The macrophage IC_{50} and casMBC potency assays used to measure drug potency at the site of disease are performed in matrices that reproduce *in vivo* drug binding and correct for protein binding. Therefore, our results are presented as total concentrations.

Limitations of our study include the fact that we studied a small sample of young children with severe forms of pulmonary TB undergoing surgery at a single site, and thus external generalizability should be evaluated further. All children were anaesthetized at the time of the procedure, and particularly those from the SD group received a significant number of concomitant drugs and intravenous fluids, all of which could have affected drug disposition. The classification of the LN histology on the fresh frozen tissue selected for PK into cellular, mixed and necrotic was challenging in some of our study samples due to freezing artefacts, absence of clear area demarcation and the fragmented nature of the tissue samples. However, routine histology samples (formalin-fixed paraffin-embedded) were usually available and provided guidance on interpretation in areas that were difficult to classify on frozen section. Finally, our PK/PD simulations in BAL should be interpreted with caution given the limited number of children in whom BAL urea concentration was successfully measured and the technical caveats such as dwelling time and volume of instilled lavage fluid.

In conclusion, we have shown that measuring the penetration of antituberculosis drugs in intrathoracic LN compartments and BAL in young children was feasible and that the penetration coefficients of first-line antituberculosis drugs into these compartments were similar to adults. The overall plasma exposures of all the drugs were low, particularly for ethambutol. Similarly, all

the first-line drugs had exposure in necrotic tissue at levels lower than current adult target concentrations. Our results indicate that current paediatric dosing guidelines do not reach target exposures at sites of disease. An improved understanding of lesion penetration, and the use of a data-driven modelling approach will allow for more-appropriate dosing in children and improved efficacy of current regimens. Our data also informs the design of novel regimens for TB treatment-shortening in children across the spectrum of pulmonary disease.

Acknowledgements

We are grateful to the children and families who participated in the study. We thank Professor Peter Donald for his comments on the manuscript and Corne Bosch and Marianna de Kock for their support in obtaining the MIC data. We thank the Sub-Saharan Africa Regional Biospecimen Repository at Tygerberg Hospital for providing liquid nitrogen and dry ice. We thank the data and clinical team from DTTC and the clinical team from Tygerberg Hospital.

Funding

This study was supported by the Spanish Ministry of Science and Innovation and State Research Agency through the 'Centro de Excelencia Severo Ochoa 2019-2023' Program (CEX2018-000806-S), and support from the Generalitat de Catalunya through the CERCA Program. E.L.V. is supported by a Spanish Paediatrics Association (AEP) fellowship and a Ramon Areces Foundation fellowship. A.A.A. and E.M.S. are supported by the European and Developing Countries Clinical Trials Partnership (EDCTP), grant number TRIA.2015.1102. J.A.S. is supported by a Clinician Scientist Fellowship jointly funded by the UK Medical Research Council (MRC) and the UK Department for International Development (DFID) under the MRC/DFID Concordat agreement (MR/R007942/1). A.M.D. is supported by National Institute of Allergy and Infectious Diseases (NIAID) of the National Institutes of Health (NIH) under Award Number UM1AI106716. A.C.H. is supported by the South African National Research Foundation (SARchi Chair), SA NRF. The funders had no role in study design, data collection and analysis, decision to publish, or preparation of the manuscript.

Transparency declarations

None to declare.

Supplementary data

Additional Methods, Figures S1 to S4 and Tables S1 to S5 are available as Supplementary data at *JAC* Online.

References

1 WHO. Global tuberculosis report 2020. https://www.who.int/publications/i/item/9789240013131.

2 Radtke KK, Dooley KE, Dodd PJ *et al*. Alternative dosing guidelines to improve outcomes in childhood tuberculosis: a mathematical modelling study. *Lancet Child Adolesc Heal* 2019; **3**: 636–45.

3 Thee S, Seddon JA, Donald PR *et al*. Pharmacokinetics of isoniazid, rifampin, and pyrazinamide in children younger than two years of age with tuberculosis: Evidence for implementation of revised World Health Organization Recommendations. *Antimicrob Agents Chemother* 2011; **55**: 5560–7.

4 Marais BJ, Gie RP, Schaaf HS *et al*. The spectrum of disease in children treated for tuberculosis in a highly endemic area. *Int J Tuberc Lung Dis* 2006; **10**: 732–8.

5 Turkova A, Wills GH, Wobudeya E *et al*. Shorter treatment for Nonsevere Tuberculosis in African and Indian children. *N Engl J Med* 2022; **386**: 911–22.

6 Prideaux B, Via LE, Zimmerman MD *et al*. The association between sterilizing activity and drug distribution into tuberculosis lesions. *Nat Med* 2015; **21**: 1223–7.

7 Strydom N, Gupta SV, Fox WS *et al*. Tuberculosis drugs' distribution and emergence of resistance in patient's lung lesions: A mechanistic model and tool for regimen and dose optimization. *PLoS Med* 2019; **16**: 1–26.

8 Zimmerman M, Lestner J, Prideaux B *et al*. Ethambutol partitioning in tuberculous pulmonary lesions explains its clinical efficacy. *Antimicrob Agents Chemother* 2017; **61**: e00924-17.

9 Dheda K, Lenders L, Magombedze G *et al*. Drug-penetration gradients associated with acquired drug resistance in patients with tuberculosis. *Am J Respir Crit Care Med* 2018; **198**: 1208–19.

10 Akkerman OW, Van Altena R, Klinkenberg T *et al*. Drug concentration in lung tissue in multidrug-resistant tuberculosis. *Eur Respir J* 2013; **42**: 1750–2.

11 Ganchua SKC, White AG, Klein EC *et al*. Lymph nodes—The neglected battlefield in tuberculosis. *PLoS Pathog* 2020; **16**: e1008632.

12 Jönsson S, Davidse A, Wilkins J *et al*. Population pharmacokinetics of ethambutol in South African tuberculosis patients. *Antimicrob Agents Chemother* 2011; **55**: 4230–7.

13 Wilkins JJ, Langdon G, McIlleron H *et al*. Variability in the population pharmacokinetics of pyrazinamide in South African tuberculosis patients. *Eur J Clin Pharmacol* 2006; **62**: 727–35.

14 Wilkins JJ, Langdon G, McIlleron H *et al*. Variability in the population pharmacokinetics of isoniazid in South African tuberculosis patients. *Br J Clin Pharmacol* 2011; **72**: 51–62.

15 Smythe W, Khandelwal A, Merle C *et al*. A semimechanistic pharmacokinetic-enzyme turnover model for rifampin autoinduction in adult tuberculosis patients. *Antimicrob Agents Chemother* 2012; **56**: 2091–8.

16 Chigutsa E, Pasipanodya JG, Visser ME *et al*. Impact of nonlinear interactions of pharmacokinetics and MICs on sputum bacillary kill rates as a marker of sterilizing effect in tuberculosis. *Antimicrob Agents Chemother* 2015; **59**: 38–45.

17 Lakshminarayana SB, Huat TB, Ho PC *et al*. Comprehensive physicochemical, pharmacokinetic and activity profiling of anti-TB agents. *J Antimicrob Chemother* 2015; **70**: 857–67.

18 Werngren J, Sturegård E, Juréen P *et al*. Reevaluation of the critical concentration for drug susceptibility testing of *Mycobacterium tuberculosis* against pyrazinamide using wild-type MIC distributions and pncA gene sequencing. *Antimicrob Agents Chemother* 2012; **56**: 1253–7.

19 Schön T, Juréen P, Giske CG *et al*. Evaluation of wild-type MIC distributions as a tool for determination of clinical breakpoints for *Mycobacterium tuberculosis*. *J Antimicrob Chemother* 2009; **64**: 786–93.

20 Rey-Jurado E, Tudó G, Soy D *et al*. Activity and interactions of levofloxacin, linezolid, ethambutol and amikacin in three-drug combinations against *Mycobacterium tuberculosis* isolates in a human macrophage model. *Int J Antimicrob Agents* 2013; **42**: 524–30.

21 Anon. Guidelines for the management of tuberculosis in children. 2013. http://www.kznhealth.gov.za/family/National-Childhood-TB-Guidelines-2013-ZA.pdf.

22 WHO. Guidance for national tuberculosis programmes on the management of tuberculosis in children. 2014. https://www.who.int/publications-detail-redirect/9789241548748.

23 Zvada SP, Denti P, Donald PR *et al*. Population pharmacokinetics of rifampicin, pyrazinamide and isoniazid in children with tuberculosis: *in silico* evaluation of currently recommended doses. *J Antimicrob Chemother* 2014; **69**: 1339–49.

24 Sturkenboom MGG, Mulder LW, De Jager A *et al*. Pharmacokinetic modeling and optimal sampling strategies for therapeutic drug monitoring of rifampin in patients with tuberculosis. *Antimicrob Agents Chemother* 2015; **59**: 4907–13.

25 Magis-Escurra C, Later-Nijland HMJ, Alffenaar JWC *et al*. Population pharmacokinetics and limited sampling strategy for first-line tuberculosis drugs and moxifloxacin. *Int J Antimicrob Agents* 2014; **44**: 229–34.

26 Abulfathi AA, Decloedt EH, Svensson EM *et al*. Clinical pharmacokinetics and pharmacodynamics of rifampicin in human tuberculosis. *Clin Pharmacokinet* 2019; **58**: 1103–29.

27 Hoff DR, Ryan GJ, Driver ER *et al*. Location of intra- and extracellular *M. tuberculosis* populations in lungs of mice and guinea pigs during disease progression and after drug treatment. *PLoS One* 2011; **6**: e17550.

28 Eshete A, Zeyinudin A, Ali S *et al*. *M. tuberculosis* in lymph node biopsy paraffin-embedded sections. *Tuberc Res Treat* 2011; **2011**: 127817.

29 Sarathy JP, Via LE, Weiner D *et al*. Extreme drug tolerance of Mycobacterium tuberculosis in caseum. *Antimicrob Agents Chemother* 2018; **62**: 1–11.

30 Gopal P, Grüber G, Dartois V *et al*. Pharmacological and molecular mechanisms behind the sterilizing activity of pyrazinamide. *Trends Pharmacol Sci* 2019; **40**: 930–40.

31 Tanner L, Haynes RK, Wiesner L. Accumulation of TB-active compounds in murine organs relevant to infection by *Mycobacterium tuberculosis*. *Front Pharmacol* 2020; **11**: 724.

32 Hiruy H, Rogers Z, Mbowane C *et al*. Subtherapeutic concentrations of first-line anti-TB drugs in South African children treated according to current guidelines: the PHATISA study. *J Antimicrob Chemother* 2014; **70**: 1115–23.

33 Donald PR, Maher D, Maritz JS *et al*. Ethambutol dosage for the treatment of children: literature review and recommendations. *Int J Tuberc Lung Dis* 2006; **10**: 1318–30.

34 Zhang N, Savic RM, Boeree MJ *et al*. Optimising pyrazinamide for the treatment of tuberculosis. *Eur Respir J* 2021; **58**: 2002013.

35 Pasipanodya JG, McIlleron H, Burger A *et al*. Serum drug concentrations predictive of pulmonary tuberculosis outcomes. *J Infect Dis* 2013; **208**: 1464–73.

36 Swaminathan S, Pasipanodya JG, Ramachandran G *et al*. Drug concentration thresholds predictive of therapy failure and death in children with tuberculosis: bread crumb trails in random forests. *Clin Infect Dis* 2016; **63**: S63–74.

37 Reynolds J, Heysell SK. Understanding pharmacokinetics to improve tuberculosis treatment outcome. *Expert Opin Drug Metab Toxicol* 2014; **10**: 813–23.

38 Guiastrennec B, Ramachandran G, Karlsson MO *et al*. Suboptimal antituberculosis drug concentrations and outcomes in small and HIV-coinfected children in India: recommendations for dose modifications. *Clin Pharmacol Ther* 2018; **104**: 733–41.

39 Rifat D, Prideaux B, Savic RM *et al*. Pharmacokinetics of rifapentine and rifampin in a rabbit model of tuberculosis and correlation with clinical trial data. *Sci Transl Med* 2018; **10**: eaai7786.

40 Garcia-Prats AJ, Svensson EM, Winckler J *et al*. Pharmacokinetics and safety of high-dose rifampicin in children with TB: the Opti-Rif trial. *J Antimicrob Chemother* 2019; **76**: 3237–46.